J Solid State Electrochem (2011) 15:747–751
DOI 10.1007/s10008-010-1151-4

ORIGINAL PAPER

Synthesis and electrochemical performance of $LiNi_{0.475}Mn_{0.475}Al_{0.05}O_2$ as cathode material for lithium-ion battery from Ni–Mn–Al–O precursor

Shumei Dou · Wen-lou Wang · Hongju Li · Xiaodong Xin

Received: 24 May 2010 / Revised: 9 July 2010 / Accepted: 16 July 2010 / Published online: 28 July 2010

Abstract $LiNi_{0.475}Mn_{0.475}Al_{0.05}O_2$ cathode material was prepared by solid-state reaction using Ni–Mn–Al–O solid solution as precursor. The solid solution is of spinel structure, in which nickel, manganese, and aluminum are sufficiently mixed at atomic level. Rietveld refinement of X-ray diffraction data revealed that Al doping in $LiNi_{0.5}Mn_{0.5}O_2$ was significantly effective to decrease the degree of Li/Ni cation mixing. XPS analysis showed that the valence states of nickel and manganese were mainly +2 and +4, respectively. $LiNi_{0.475}Mn_{0.475}Al_{0.05}O_2$ delivered a stable capacity of about 206 mAh g^{-1} with high reversibility. High-rate capability test was also performed.

Keywords Lithium-ion battery · $LiNi_{0.475}Mn_{0.475}Al_{0.05}O_2$ · Solid solution · Solid-state reaction · Precursor · Electrochemical properties

Introduction

Layered lithium nickel manganese oxides are the alternative to the commercial $LiCoO_2$ electrode materials used in lithium-ion batteries due to their inexpensive and nontoxic properties. Among these, $LiNi_{0.5}Mn_{0.5}O_2$ is one of the most attractive materials [1–7]. Various synthesis methods have been applied to prepare this material. However, it is known that the high battery-active $LiNi_{0.5}Mn_{0.5}O_2$ is not easy to obtain due to it either containing structural impurities or existing substantial Li/Ni cation mixing. Recently, many research groups have solved these problems by co-precipitation or ion-exchange methods. However, the former needs to be operated carefully to control the synthesis conditions since Mn^{2+} can be easily oxidized in air, and the latter consumes a large amount of salts containing Li^+.

However, the performance of $LiNi_{0.5}Mn_{0.5}O_2$ cathode materials can be improved by doping transition metal ions or nontransition metal ions. Aluminum is a commonly used dopant in cathode materials. In some cases, small amounts of aluminum doping improve the capacity of the $LiNi_{0.5}Mn_{0.5}O_2$ [8–10] since Al^{3+} can improve electrode kinetics, structure modifications, and microstructural effects [11]. However, in most cases, the capacity decreased [12] because Al^{3+} cannot deliver capacity. In addition, it is found that doping Ti in $LiNi_{0.5}Mn_{0.5}O_2$ with a different method can play a different role in the electrochemical performance [13, 14]. Therefore, the doping method is also an important factor of affecting the electrochemical performance.

In our previous work, $LiNi_{0.5}Mn_{0.5}O_2$ cathode materials that were prepared using Ni–Mn–O solid solution as precursor succeeded in reducing cation mixing since the distribution of nickel and manganese is homogeneous at the atomic level in the solid solution [15]. This method did not need a multistep process or complex conditions, and it can be used to prepare high battery-active cathode materials in a large scale. In the present work, we synthesized $LiNi_{0.475}Mn_{0.475}Al_{0.05}O_2$ cathode materials by solid-state reaction method using Ni–Mn–Al–O solid solution as precursor.

S. Dou · W.-l. Wang (✉) · H. Li · X. Xin
Department of Chemical Physics,
University of Science and Technology of China,
Hefei, Anhui 230026, People's Republic of China
e-mail: wlwang@ustc.edu.cn

Experimental

Synthesis

Mixture of Mn $(CH_3COO)_2$ $4H_2O$ (AR, 99%), Ni $(CH_3COO)_2{\cdot}4H_2O$ (AR, 98%), and Al $(NO_3)_3{\cdot}9H_2O$ (AR, 99%) with a molar ratio of 0.475:0.475:0.05 was completely dissolved in distilled water. Water was removed by means of a rotary evaporator at 75°C, and then salt precipitate was made. The salt precipitate was ground and calcined at 800°C for 12 h in air. The as-prepared precursor was mixed with $LiOH{\cdot}H_2O$ (AR, 99%) in stoichiometric proportion and then pressed into pellets. The pellets were heated at 550°C for 3 h, followed by annealing at 900°C for 12 h in air. The pellets were quenched to room temperature using a copper plate.

Characterization

Powder X-ray diffraction (XRD) was performed on a Philips X'pert pro X-ray diffractometer equipped with graphite monochromatized high-intensity Cu Kα radiation (λ=1.54178) in the 2θ range from 10° to 80°. The contents of cations in precursor were measured by inductively coupled plasma atomic analysis (ICP, Atomscan Advantage). The scanning electron microscope (SEM) study of the samples was performed using JEOL JSM-6700F electron microscope.

Charge and discharge profiles were collected by galvanostatically cycling between 2.5 and 4.4 V on multi-channel battery testers (Shenzhen Neware, BTS, China). For the preparation of cathode sheets, slurry was formed by mixing the active material, acetylene black, and binder (polyvinylidene fluoride (PVDF) dissolved in *N*-methyl-2-pyrrolidone (NMP)) in a weight ratio of 75:20:5. The slurry was spread uniformly on aluminum foil. The electrodes were dried under vacuum at 120°C overnight and then punched and weighed. One mole of LiPF6 in a 1:1 ethylene carbonate/diethyl carbonate was used as electrolyte, and lithium foil was used as anode. A thin sheet of microporous polypropylene insulated the cathode from lithium foil anode. Battery assembly was carried out in an argon-filled glove box. Cyclic voltammetry (CV) was measured on an electrochemical workstation (CHI660C, Shanghai, China) at a scanning rate of 0.1 mV s^{-1} between 2.5 and 4.4 V (vs Li/Li^+).

Results and discussion

Figure 1 shows the XRD pattern of as-prepared precursor Ni–Mn–Al–O solid solution, which is similar to the pattern of $NiMn_2O_4$ (JCPDS 84-0542). All the peaks can be indexed to the Fd3m space with a cubic lattice. The chemical compositions of as-prepared precursor were determined by ICP, and the results are summarized in Table 1. The measured cation ratios of Ni:Mn:Al are well in agreement with the intended composition. The XRD pattern and the chemical compositions of the precursor imply that the metal oxide is homogeneously reacted, ensuring sufficient mixing of Ni–Mn–Al in the precursor at the atomic level.

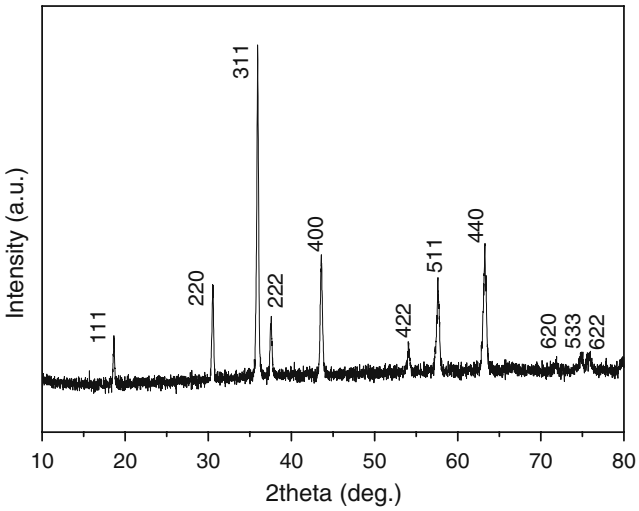

Fig. 1 XRD pattern of Ni–Mn–Al–O solid solution precursor

The morphology of the precursor and final sample $LiNi_{0.475}Mn_{0.475}Al_{0.05}O_2$ is shown in Fig. 2. The precursor has a uniform structure morphology and porous crystal surface with narrow size distribution less than 1 μm. The final sample has an irregular morphology with smooth crystal surface, and the size distribution is broader than that of the precursor but narrower than that of $LiNi_{0.5}Mn_{0.5}O_2$ prepared with the same method [15]. Therefore, the microstructure can be affected by the dopant additions of aluminum, similar to the aluminum-doping $LiCoO_2$ [16].

The XRD pattern of the final sample $LiNi_{0.475}Mn_{0.475}Al_{0.05}O_2$ and the observed, calculated, and difference diffraction profiles of $LiNi_{0.475}Mn_{0.475}Al_{0.05}O_2$ for rietveld refinement using the XRD pattern are shown in Fig. 3. The initial model is that of $LiNi_{0.475}Mn_{0.475}Al_{0.05}O_2$ with space group $R\bar{3}m$ and atomic position Li1/Ni1 at 3a(0,0,0), Li2/Ni2/Mn/Al at 3b(0,0,0.5) and O at 6c (0,0,z), where z is also refined. During Rietveld refinement, the occupancy of the 3b site by Mn and Al was maintained at 0.475 and 0.05, respectively, and the total amount of Li and Ni within the material was fixed; however, the distribution of Li and Ni between the 3a and 3b sites was allowed to vary. The

Table 1 Chemical composition (wt%) of the prepared precursor determined by ICP

Ni	Mn	Al	Molar ratio of Ni:Mn:Al
30.79	28.70	1.69	0.473:0.471:0.056

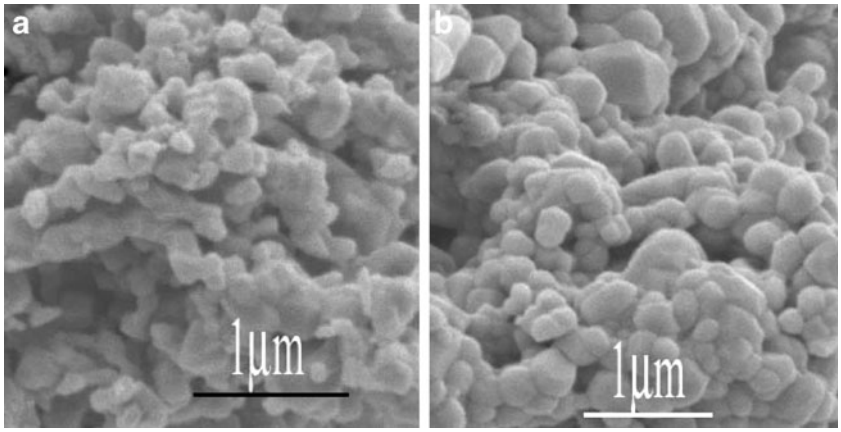

Fig. 2 SEM images of precursor (**a**) and $LiNi_{0.475}Mn_{0.475}Al_{0.05}O_2$ (**b**)

refinement converged on a model in which 5.6 mol% of the Ni ions in the 3b sites were exchanged for Li, less than the 7.5% for the sample without Al doping as our group synthesized. This model provided an excellent fit to the data, as can be seen in Fig. 3, corresponding to Rwp and Rp of 5.21% and 4.15%, respectively. Refined unit-cell parameters, in a hexagonal setting, were a=2.891 and c=14.321 Å. The lattice parameter, c, correlated to the average metal–metal inter-slab distance, is longer than those reported previously [8, 10, 17], similar to the addition of aluminum to $LiCoO_2$ [18, 19]. The increase in lattice parameter c can facilitate lithiation and delithiation [10].

In order to confirm the oxidation state of the transition metal species in the synthesized $LiNi_{0.475}Mn_{0.475}Al_{0.05}O_2$, an XPS study was carried out and is shown in Fig. 4. In the Ni XPS spectra, a characteristic satellite peak centered at 860.8 eV is noted in addition to the Ni $2p_{3/2}$ peak. Such a satellite peak was also observed in NiO, $LiNiO_2$, $LiNi_{1/3}Mn_{1/3}Co_{1/3}O_2$, and $LiNi_{0.5}Mn_{1.5}O_4$ [20–23] and was explained as being due to multi-electron excitation [21, 22]. The peak with binding energy 854.5 eV agrees with those reported for Ni^{2+} [22, 24]. In addition, the best fit for Ni $2p_{3/2}$ spectrum givens one binding energy values as shown in the insert. As shown in Fig. 4b, the binding energy of the Mn 2p XPS spectra is

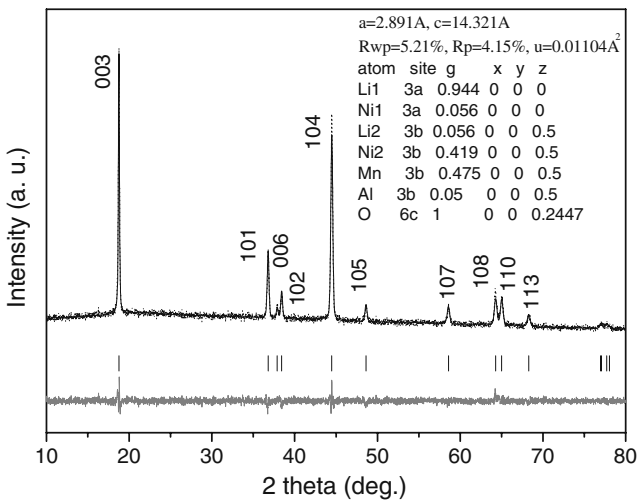

Fig. 3 Observed, calculated, and difference diffraction profiles of $LiNi_{0.475}Mn_{0.475}Al_{0.05}O_2$ for Rietveld refinement

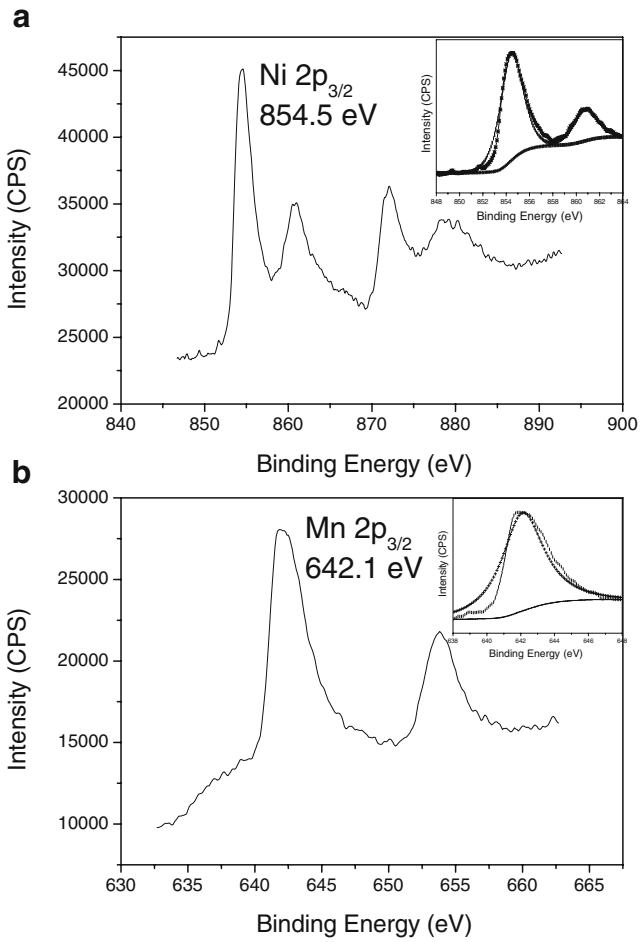

Fig. 4 XPS of **a** Ni 2p, **b** Mn 2p of the $LiNi_{0.475}Mn_{0.475}Al_{0.05}O_2$ (the *insets* in **a** and **b** are the best fit for the spectrum, respectively)

642.1 eV, which consists of the Mn $2p_{3/2}$ in λ-MnO_2 [21]. Similar to the Ni $2p_{3/2}$, the Mn $2p_{3/2}$ spectrum also gives one peak for its best fit. Therefore, the valence state of Mn in $LiNi_{0.475}Mn_{0.475}Al_{0.05}O_2$ is +4. The XPS results are in accordance with the results reported elsewhere [8].

CV of $LiNi_{0.475}Mn_{0.475}Al_{0.05}O_2$ sample was tested in the potential region of 2.5–4.4 V shown in Fig. 5. There are no redox peaks around 3 V in the CV curves, indicating that Mn ions in the sample are electrochemically inactive and present the valence state of +4. The observed peaks around 4 V are attributed to the redox reaction of Ni^{2+}/Ni^{4+} [6, 24]. Therefore, the valence states of Ni and Mn are +2 and +4, respectively, agreeing with the results of the XPS analysis. The oxidation and reduction peaks are located at 4.08 and 3.73 V, respectively, which are higher than those of $LiNi_{0.5}Mn_{0.5}O_2$ [14]. In addition, the differential peak potential Δφ is about 0.35 V, smaller than those of $LiNi_{0.5}Mn_{0.5}O_2$ reported by Kang [24], demonstrating the better reversibility of the intercalation and deintercalation of lithium ions in the electrode materials.

The initial, second, third, fifth, 10th, 20th, and 30th cycle charge–discharge curves of $LiNi_{0.475}Mn_{0.475}Al_{0.05}O_2$ are shown in Fig. 6a. The cell was operated in the voltage range from 2.5 to 4.4 V at a rate of 20 mA g^{-1}. There is only one voltage plateau on both charge and discharge curves, which is consistent with the results in CV experiments. The ratio of initial discharge/charge is about 96%. From the second to the 30th cycle, the ratios of discharge/charge are larger than 98%, illuminating that the electrochemical reversibility was established after the initial cycle. As shown in Fig. 6b, the batteries show about 202 mAh g^{-1} of rechargeable capacity without dramatic capacity fading during 30 cycles, with only 2.0% capacity decreased. This result indicates that the designed cathode material with high capability has a high degree of cation ordering required for good Li^+ mobility [25].

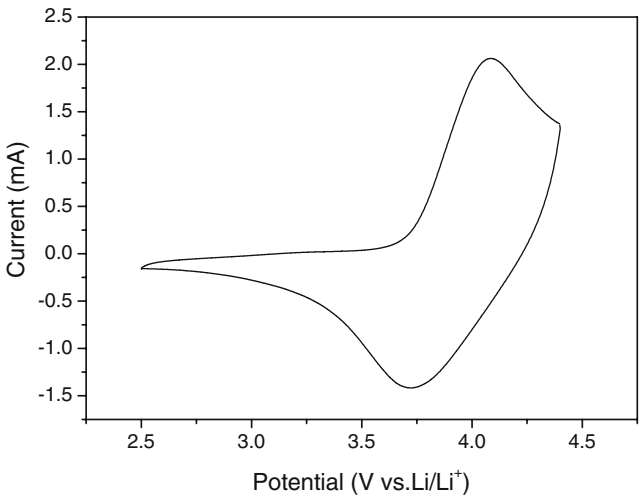

Fig. 5 Cyclic voltammetry of the synthesized $LiNi_{0.475}Mn_{0.475}Al_{0.05}O_2$ in the voltage range 2.5–4.4 V at scanning rate 0.1 mV s^{-1}

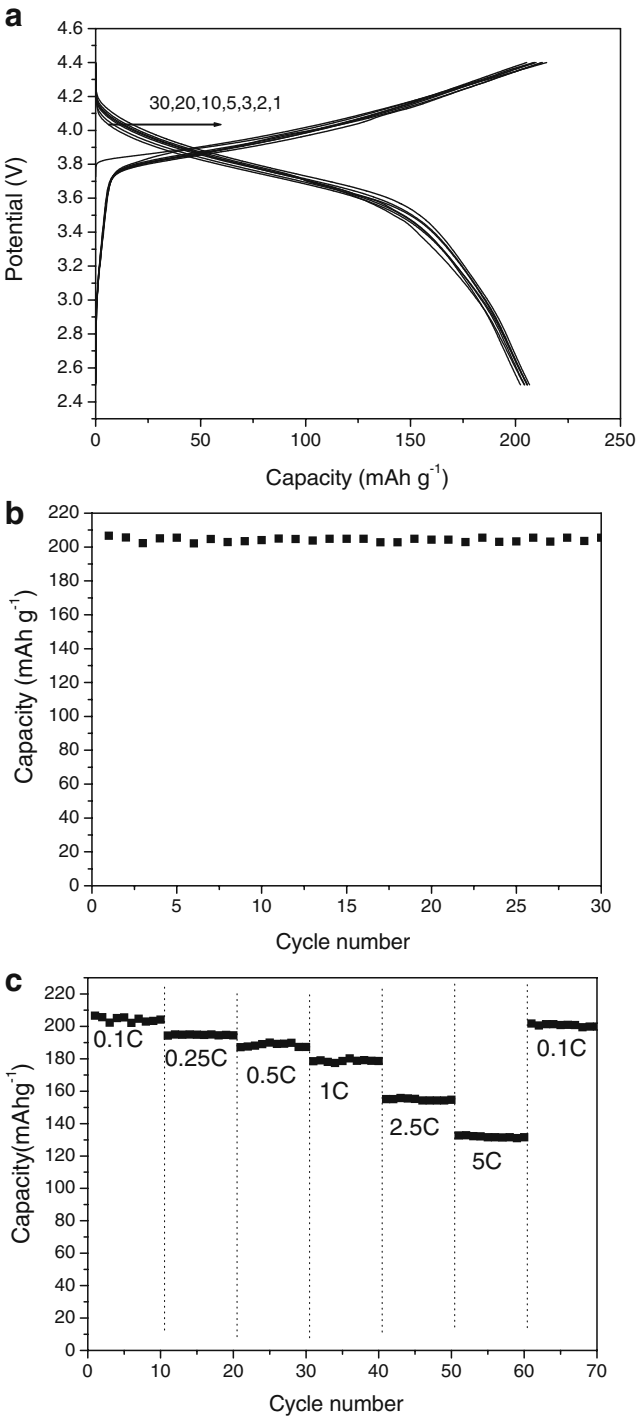

Fig. 6 **a** Charge and discharge curves of the synthesized $LiNi_{0.475}Mn_{0.475}Al_{0.05}O_2$ in the voltage from 2.5 to 4.4 V at a rate of 20 mA g^{-1}. **b** Charge and discharge capacity as a function of cycle number. **c** Discharge capacity at different current with cycle number. The charge rate was fixed at 0.1 C (20 mA g^{-1})

Rate capability is one of the important electrochemical characteristics of a lithium-ion battery required for power

storage application. In the present study, to investigate the effect of Al doping on the rate capability, a cell with $LiNi_{0.475}Mn_{0.475}Al_{0.05}O_2$ as the cathode materials was cycled between 2.5 and 4.4 V at different discharge current densities: 0.1 C, 0.25 C, 0.5 C, 1C, 2.5 C, and 5 C (1 C=200 mAh g^{-1}), respectively. As can be seen in Fig. 6c, for every 10 cycles at the same rate, the rate capacities scarcely changed. Even after 10 cycles at the rate of 5 C, 131.5 mAh g^{-1} capacity remained. After completion of the high rate test, the capacity is still about 200 mAh g^{-1}, which is almost its original value, indicating that the as-prepared $LiNi_{0.475}Mn_{0.475}Al_{0.05}O_2$ material has good electrochemical reversibility and structure stability. The rate capability suggests that the synthesized $LiNi_{0.475}Mn_{0.475}Al_{0.05}O_2$ material would be well suitable for cathode materials of high-power lithium batteries.

Conclusion

Layered structured $LiNi_{0.475}Mn_{0.475}Al_{0.05}O_2$ sample was synthesized by solid state reaction using Ni–Mn–Al–O solid solution as precursor. The distribution of Ni, Mn, and Al is homogeneous at the atomic level in the solid solution, which results in highly ordering of cations in the final sample $LiNi_{0.475}Mn_{0.475}Al_{0.05}O_2$. Aluminum doping narrows the size distribution, lengthens the lattice parameter *c*, and reduces the degree of Li/Ni cations' mixing. The XPS and CV data suggest that Ni and Mn are present as Ni^{2+} and Mn^{4+}, respectively. The electrochemical performance indicates that $LiNi_{0.475}Mn_{0.475}Al_{0.05}O_2$ prepared in this study has a competitive capacity, cycle ability, and rate capability, indicating that the $LiNi_{0.475}Mn_{0.475}Al_{0.05}O_2$ can be used as a possible alternative to $LiCoO_2$.

Acknowledgements This work was supported by a grand from Natural Science Foundation of Anhui Province (Grant No. 090414178).

References

1. Ohzuku T, Majumura Y (2001) Chem Lett 30:744–745
2. Makimura Y, Ohzuku T (2003) J Power Sources 119–121:156–160
3. Kang K, Meng YS, Breger J, Grey CP, Ceder G (2006) Science 311:977–980
4. Hinuma Y, Meng YS, Kang K, Ceder G (2007) Chem Mater 19:1790–1800
5. Lu Z, MacNeil DD, Dahn JR (2001) Electrochem Solid-State Lett 4:A191–A194
6. Lu Z, Beaulieu LY, Donaberger RA, Thomas CL, Dahn JR (2002) J Electrochem Soc 149:A778–A791
7. Chou J, Kim Y, Kim G (2007) J Phys Chem C 111:3192–3196
8. Zhang B, Chen G, Xu P, Li CC (2008) J Power Sources 176:325–331
9. Komaba S, Yoshii K, Ogata A, Nakai I (2009) Electrochim Acta 54:2353–2359
10. Zhang B, Chen G, Liang Y, Xu P (2009) Solid State Ionics 180:398–404
11. Fergus JW (2010) J Power Sources 195:939–954
12. Zhou F, Zhao X, Lu Z, Jiang J, Dahn JR (2008) Electrochem Solid-State Lett 11:A155–A157
13. Li DC, Muta T, Noguchi H (2004) J Power Sources 135:262–266
14. Li D, Noguchi H (2003) ITE Lett Batter New Technol Med 4:303–307
15. Meng XL, Dou SM, Wang W-L (2008) J Power Sources 184:489–493
16. Ju SH, Jang HC, Kang YC (2008) Mater Chem Phys 112:536–541
17. Myung S-T, Komaba S, Hirosaki N, Hosoya K, Kumagai N (2005) J Power Sources 146:645–649
18. Luo W, Dahn JR (2009) Electrochim Acta 54:4655–4661
19. Luo W, Dahn JR (2009) Chem Mater 21:56–62
20. Shaju KM, Subba Rao GV, Chowdari BVR (2002) Electrochim Acta 48:145–151
21. Carley AF, Jackson SD, O'Shea JN, Roberts MW (1999) Surf Sci 440:L868–L874
22. Amine K, Tukamoto H, Yasuda H, Fujita Y (1996) J Electrochem Soc 143:1607–1613
23. Mansour AN (1996) Surf Sci Spectra 3:279–286
24. Kang SH, Kim J, Stoll ME, Abraham D, Sun YK, Amine K (2002) J Power Sources 112:41–48
25. Schougaard B, Breger J, Jiang M, Grey CP, Goodenough JB (2006) Adv Mater 18:905–909